

UNCLASSIFIED

AD NUMBER

ADB012784

LIMITATION CHANGES

TO:

Approved for public release; distribution is unlimited.

FROM:

Distribution authorized to U.S. Gov't. agencies only; Test and Evaluation; 12 AUG 2009. Other requests shall be referred to Army Research Laboratory, Attn: ARL-APG Security Office, RDRL-LOA-I, Aberdeen Proving Ground, MD 21005.

AUTHORITY

UAARDC ltr, 8 Mar 1978

THIS PAGE IS UNCLASSIFIED

AD-B 012 784

USADAC TECHNICAL LIBRARY



5 0712 01017825 8

BRL MR

BRL

AD

TECHNICAL
LIBRARY

MEMORANDUM REPORT NO. 2646

MUZZLE-BLAST INFLUENCE ON TRAJECTORY OF
ASYMMETRICAL FIN-STABILIZED PROJECTILES

Kevin S. Fansler
Edward M. Schmidt

August 1976

19971010 121

Distribution limited to US Government agencies only; Test and
Evaluation; Aug '76. Other requests for this document must be
referred to Director, USA Ballistic Research Laboratories,
ATTN: DRXBR-TS, Aberdeen Proving Ground, Maryland 21005.

DTIC QUALITY INSPECTED 8

USA BALLISTIC RESEARCH LABORATORIES
ABERDEEN PROVING GROUND, MARYLAND

Destroy this report when it is no longer needed.
Do not return it to the originator.

Secondary distribution of this report by originating
or sponsoring activity is prohibited.

Additional copies of this report may be obtained
from the Defense Documentation Center, Cameron
Station, Alexandria, Virginia 22314.

The findings in this report are not to be construed as
an official Department of the Army position, unless
so designated by other authorized documents.

THIS REPORT HAS BEEN DELIMITED
AND CLEARED FOR PUBLIC RELEASE
UNDER DOD DIRECTIVE 5200.20 AND
NO RESTRICTIONS ARE IMPOSED UPON
ITS USE AND DISCLOSURE.

DISTRIBUTION STATEMENT A

APPROVED FOR PUBLIC RELEASE;
DISTRIBUTION UNLIMITED.

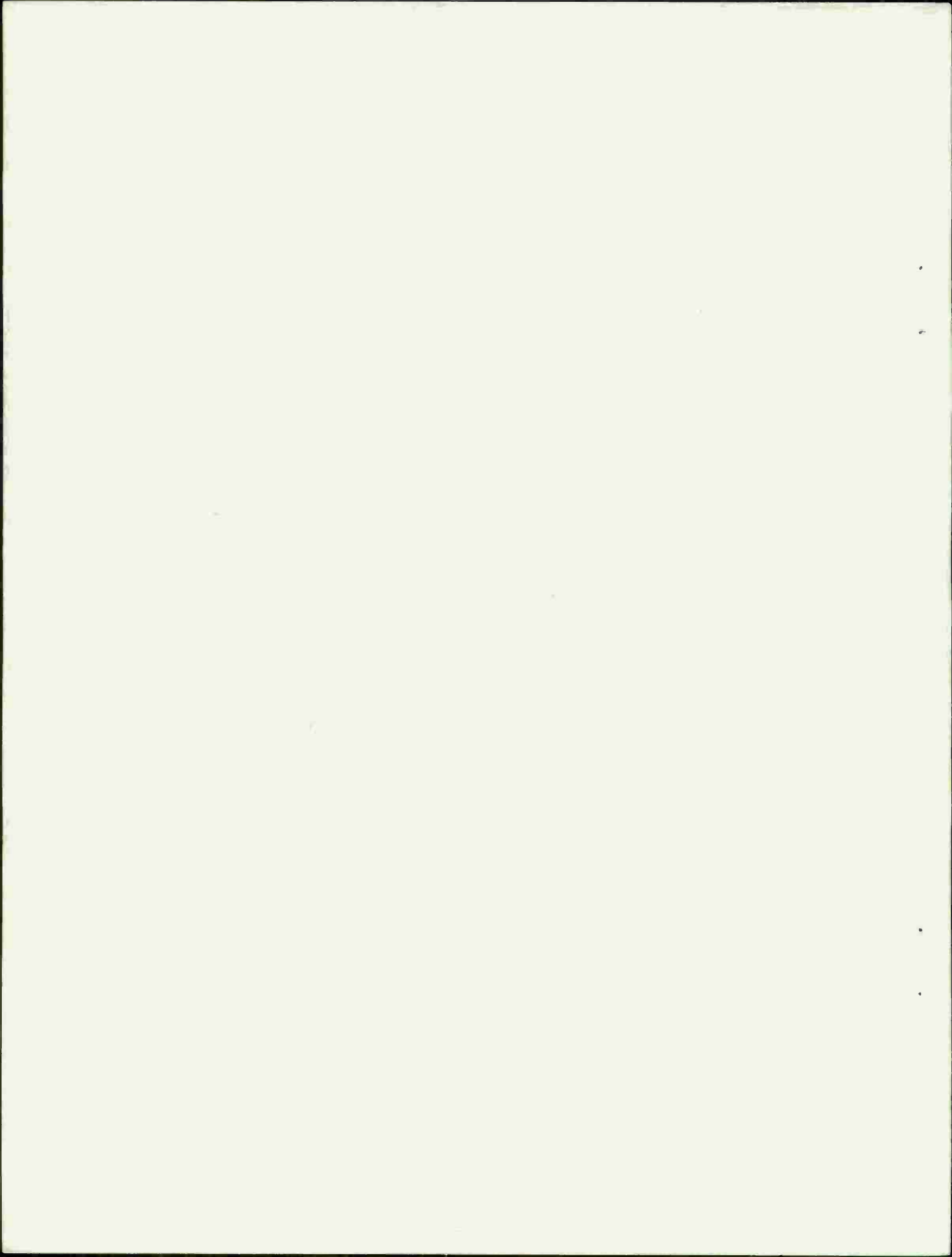
UNCLASSIFIED

SECURITY CLASSIFICATION OF THIS PAGE (When Data Entered)

REPORT DOCUMENTATION PAGE		READ INSTRUCTIONS BEFORE COMPLETING FORM
1. REPORT NUMBER BRL Memorandum Report No. 2646	2. GOVT ACCESSION NO.	3. RECIPIENT'S CATALOG NUMBER
4. TITLE (and Subtitle) MUZZLE-BLAST INFLUENCE ON TRAJECTORY OF ASYMMETRICAL FIN-STABILIZED PROJECTILES		5. TYPE OF REPORT & PERIOD COVERED
		6. PERFORMING ORG. REPORT NUMBER
7. AUTHOR(s) Kevin S. Fansler and Edward M. Schmidt		8. CONTRACT OR GRANT NUMBER(s)
9. PERFORMING ORGANIZATION NAME AND ADDRESS USA Ballistic Research Laboratories Aberdeen Proving Ground, Maryland 21005		10. PROGRAM ELEMENT, PROJECT, TASK AREA & WORK UNIT NUMBERS RDT&E 1W161102AH43
11. CONTROLLING OFFICE NAME AND ADDRESS U.S. Army Materiel Development and Readiness Command, 5001 Eisenhower Avenue, Alexandria, Virginia 22333		12. REPORT DATE AUGUST 1976
		13. NUMBER OF PAGES 30
14. MONITORING AGENCY NAME & ADDRESS (if different from Controlling Office)		15. SECURITY CLASS. (of this report) UNCLASSIFIED
		15a. DECLASSIFICATION/DOWNGRADING SCHEDULE
16. DISTRIBUTION STATEMENT (of this Report) Distribution limited to US Government agencies only; Test and Evaluation; August 1976. Other requests for this document must be referred to Director, USA Ballistic Research Laboratories, ATTN: DRXBR-TS, Aberdeen Proving Ground, MD 21005.		
17. DISTRIBUTION STATEMENT (of the abstract entered in Block 20, if different from Report)		
18. SUPPLEMENTARY NOTES		
19. KEY WORDS (Continue on reverse side if necessary and identify by block number) Fin-stabilized Projectiles Free-Flight Ballistics Transitional Ballistics Projectile Accuracy		
20. ABSTRACT (Continue on reverse side if necessary and identify by block number) (ner) Trajectory perturbations caused by muzzle blast are investigated by analytical techniques. A closed-form expression for the deflection of the projectile is obtained. Using this expression, it is found that the jump caused by muzzle blast is negligible compared to the total dispersion.		

TABLE OF CONTENTS

	<u>Page</u>
LIST OF ILLUSTRATIONS.	5
I. INTRODUCTION	7
II. ANALYSIS OF GASDYNAMIC LOADINGS.	8
III. THE JUMP EQUATIONS	13
IV. APPROXIMATION OF ϕ_t	15
V. DEVIATION CAUSED BY MUZZLE BLAST ON ASYMMETRIC PROJECTILES .	19
VI. SUMMARY AND CONCLUSIONS.	22
ACKNOWLEDGMENT	22
REFERENCES	23
LIST OF SYMBOLS	25
DISTRIBUTION LIST	27



LIST OF ILLUSTRATIONS

<u>Figure</u>	<u>Page</u>
1. Sources of Gasdynamic Loadings During Launch.	9
2. Comparison of Inbore and Muzzle-Jet Impulse [for $d/D = 1$]	10
3. Coordinate Systems	11
4. Illustrating Differential Fin Cant	12
5. Magnitude of ϕ_t versus $\phi_\infty' C^{-1}$	18
6. Argument of ϕ_t versus $\phi_\infty' C^{-1}$	19

I. INTRODUCTION

Aerodynamic or inertial asymmetry of a fin-stabilized non-rolling projectile results in the round's trimming to a fixed attitude once launch disturbances damp out. This preferential trim produces a continuously increasing divergence of the flight path from the intended trajectory. To avoid this effect, the projectile is given some small roll rate, either in-bore or in free flight. The trajectory of a rolling projectile still suffers an aerodynamic jump due to the asymmetry, but the continuous divergence is eliminated. Murphy and Bradley¹ have demonstrated that the magnitude and direction of the aerodynamic jump are related not only to the steady-state roll rate but also to the variation in roll rate between launch and steady-state values. Their analysis assumes that the projectile enters free flight with roll rate equal to its in-bore value. This assumption neglects the perturbation of the roll due to transit of the muzzle blast.

To produce a rolling moment on a fin-stabilized projectile, differential fin cant is generally used. In the reverse flow of the muzzle blast, the direction of the rolling moment is opposite to that in free flight. As a result, the roll rate decreases from the launch value. For projectiles fired from smoothbore guns, a reverse spin may be produced. Fansler and Schmidt² extended the computations of Murphy and Bradley¹ to include the case of projectiles spinning up to a positive free flight value from an initially negative roll rate. Additionally, Fansler and Schmidt calculated the transverse linear and angular momentum imparted by the muzzle blast to a projectile with an

-
1. C. H. Murphy and J. W. Bradley, "Jump Due to Aerodynamic Asymmetry of a Missile with Varying Roll Rate," BRL R 1077, U. S. Army Ballistic Research Laboratories, Aberdeen Proving Ground, Maryland, May 1959, AD 219312.
 2. K. S. Fansler and E. M. Schmidt, "The Influence of Muzzle Gas-dynamics upon the Trajectory of Fin-Stabilized Projectiles," BRL R 1793, U. S. Army Ballistic Research Laboratories, Aberdeen Proving Ground, Maryland, June 1975, AD B005379L.

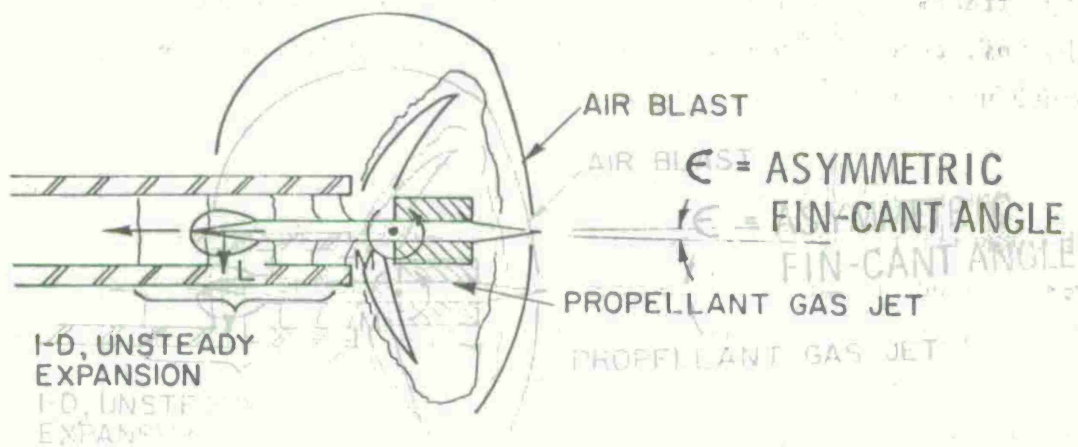
aerodynamic asymmetry. In a sample case, they demonstrated that the increase in jump due to negative roll rate is cancelled by the component of jump due to the projectile transverse velocities imparted by the muzzle blast. However, since the integration of the equations of motion was performed numerically, a closed-form solution was not obtained, and no general statement regarding this cancellation effect could be made.

The present report used an analytical approach to obtain a closed-form expression for the jump of a slightly asymmetric, fin-stabilized projectile due to muzzle blast. The flow is modelled using a quasi-steady approximation² which provides for direct evaluation of the gas-dynamic forces on the projectile during launch. From the resulting loading history, the motion of the projectile through the muzzle blast and into free flight is determined. Once the initial dynamics of the round are known, its subsequent trajectory may be obtained by numerically integrating the equations of motion^{1,2}. In the present report, the expression for the trajectory deflection due to asymmetry is expanded as a Taylor series and compared to the results of the numerical integration. Substitution of this series into the jump equation provides a general prediction of the muzzle-blast-induced jump of asymmetric projectiles.

II. ANALYSIS OF GASDYNAMIC LOADINGS

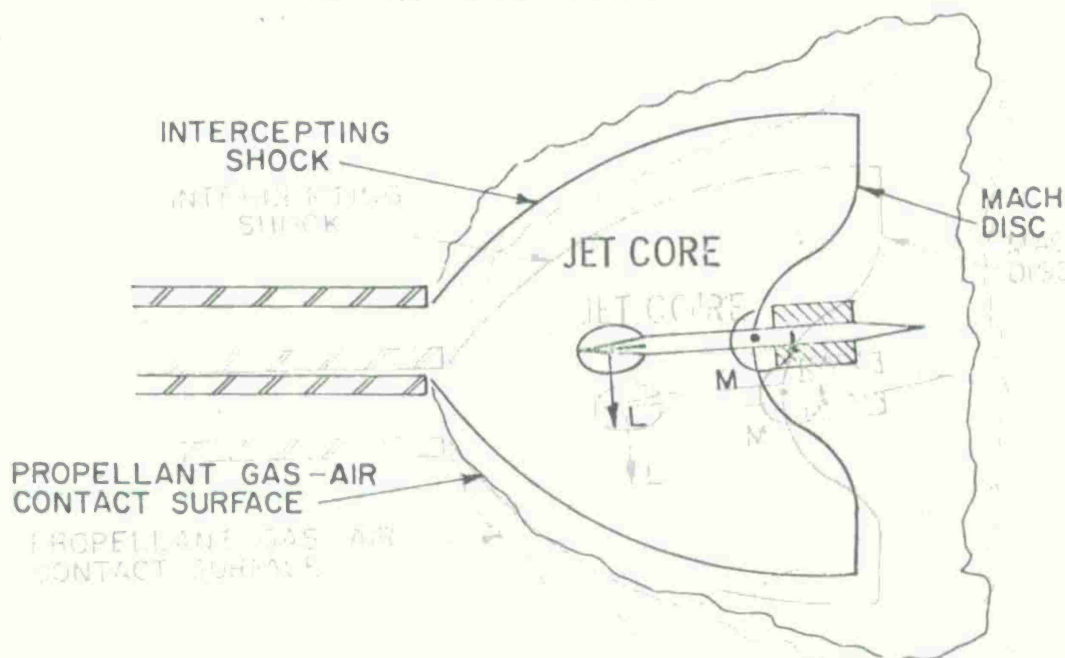
At launch, a fin-stabilized projectile is subject to gasdynamic loadings in two distinct muzzle flows: the in-bore expansion and the muzzle blast, Figure 1. In this report, the analysis of Fansler and Schmidt² is used to describe the muzzle flow. They modelled the in-bore flow as a one-dimensional, unsteady expansion and the external flow as a quasi-steady³, axially symmetric jet flow. Transverse gas-

3. K. Oswatitsch, "Intermediate Ballistics," *Deutsche Luft und Raumfahrt* FB 64-37, DVL Bericht 358, December 1964, AD 473249.



A. IN-BORE PHASE

A. IN-BORE PHASE



B. MUZZLE JET PHASE

B. MUZZLE JET PHASE

Figure 1. Sources of Gasdynamic Loadings During Launch

Figure 1. Sources

dynamic loads are assumed to be generated only upon fin surfaces⁴. These loadings are computed from the local flow properties and two-dimensional, thin airfoil theory without correcting for flow inclination, tip effects, or wing-body interference. These approximations eliminate the influence of fin and projectile geometry and produce an upper bound upon muzzle blast loadings.

Using this model, the loadings upon the fins may be integrated through the muzzle blast to obtain an expression for the momentum transferred to the projectile. Fansler and Schmidt² determined non-dimensional impulse functions that are independent of the projectile and flow geometry and vary only with propellant gas Mach number prior to shot ejection, V_p/c_1 , Figure 2. Here V_p is the projectile

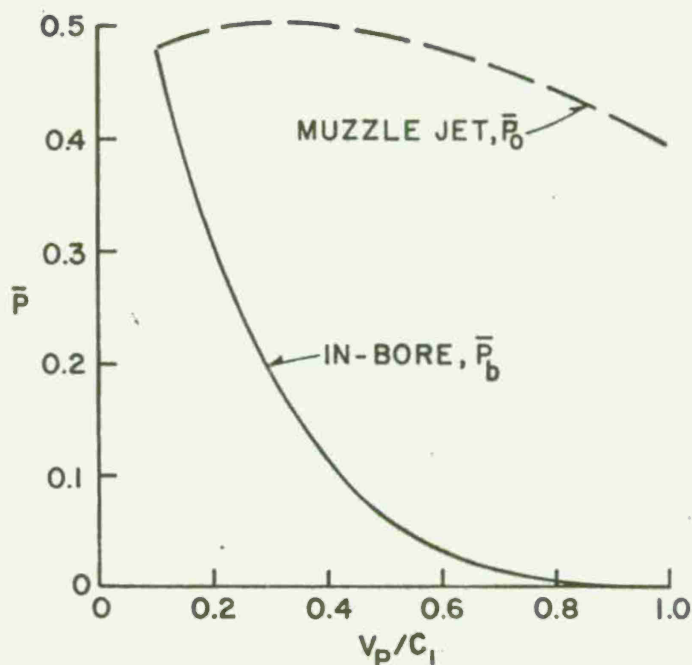


Figure 2. Comparison of In-bore and Muzzle-Jet Impulse
[for $d/D = 1$]

4. W. Gretler, "Intermediate Ballistics Investigations of Wing Stabilized Projectiles," German Air and Space Research Report 67-92, FSTC-HT-23-22-69-72, 1967.

velocity and c_1 is the prelaunch propellant gas speed of sound. The total impulse is the sum of the in-bore and muzzle jet function values, $\bar{P} = \bar{P}_0 + (d/D) \bar{P}_b$. Here d is the distance from obturator to fin and D is the gunbore diameter. This function is used to calculate the transverse angular and linear velocities and reverse spin imparted to the projectile during transit of the muzzle gases.

The coordinate systems used in this report are standard in ballistic calculations¹, Figure 3. The nonrolling coordinates are

x_e, y_e, z_e - EARTH FIXED SYSTEM

$\tilde{x}, \tilde{y}, \tilde{z}$ - MISSILE FIXED, NON-ROLLING SYSTEM

$\tilde{\alpha}, \tilde{\beta}$ - ANGLES OF ATTACK AND SIDESLIP RESPECTIVELY

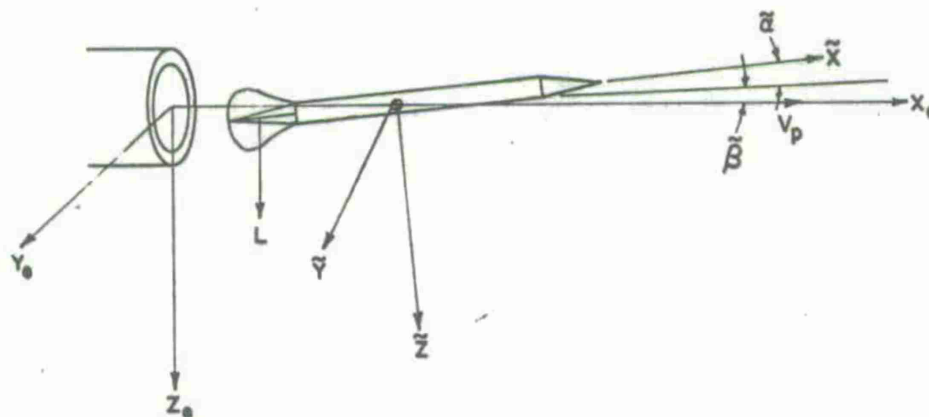


Figure 3. Coordinate Systems

used to describe the projectile angular motion, while the earth-fixed coordinates are employed in the solution for projectile jump. At separation from the gun, the projectile velocity vector is assumed to lie along the x_e axis. Since it is of interest to examine muzzle blast effects caused by asymmetry, we assume

$$\tilde{\alpha}_m = \tilde{\beta}_m = \tilde{\alpha}_m' = \tilde{\beta}_m' = \frac{w_m}{V_p} = \frac{v_m}{V_p} \equiv 0$$

where the subscript m refers to values immediately at separation. Here the prime superscript denotes rate of change of the variable with respect to distance in calibers traveled by the projectile. Further, we restrict the analysis to projectiles launched from smooth-bore guns:

$$\phi'_m \equiv 0.$$

For simplicity, the aerodynamic asymmetry to be treated is postulated as two opposing fins, inclined at an angle, ϵ (in the same sense for both fins) with respect to their normal orientation. The differential fin cant angle, 2δ , Figure 4, between opposing fins

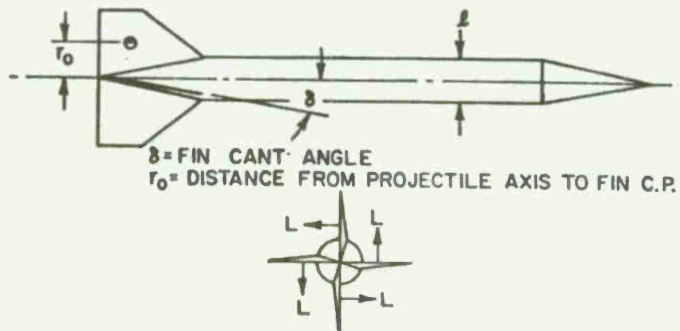


Figure 4. Illustrating Differential Fin Cant

is unaltered and the steady state roll rate, ϕ'_∞ is maintained. The transverse linear velocity imparted to the projectile in the muzzle flow is computed² to be:

$$\frac{v_o}{V_p} + i \frac{w_o}{V_p} = (\gamma + 1) p^* 2A_f \frac{D}{M_p V_p^2} \bar{P} (\epsilon e^{i(\phi_\epsilon + \pi)}), \quad (1)$$

where

- ϕ_ϵ = initial orientation of asymmetric force in free flight.
- v_o = muzzle-blast imparted velocity in Y_e direction
- w_o = muzzle-blast imparted velocity in Z_e direction
- p^* = pressure at muzzle for critical conditions

$\phi_\epsilon + \pi$ = orientation of asymmetric force in the muzzle jet

A_f = plan area of one fin

M_p = mass of projectile

The transverse angular velocity is

$$\tilde{\xi}'_0 = \tilde{\beta}'_0 + i \tilde{\alpha}'_0 = (\gamma+1) p^* 2A_f \frac{\Delta D \ell}{I_y V_p^2} \bar{p} (\epsilon e^{i(\phi_\epsilon + \pi)}), \quad (2)$$

where

I_y = transverse moment of inertia

Δ = moment arm of force on fins about the center of gravity.

Finally, the reverse spin imparted by the muzzle blast due to differential fin cant with an equivalent moment arm length r_0 is

$$\phi'_0 = -(\gamma+1) p^* n A_f \frac{r_0 D \ell}{I_x V_p^2} \bar{p} \delta \quad (3)$$

where

I_x = axial moment of inertia

δ = angle of differential fin cant

III. THE JUMP EQUATIONS

The dynamic state of the projectile upon leaving the muzzle blast region and entering into free flight defines its subsequent trajectory permitting the computation of jump due to muzzle-gas effects. The deviation from its intended trajectory is

$$\Theta = \lim_{X_e \rightarrow \infty} \frac{Y_e + i Z_e}{X_e} \quad (4)$$

where the coordinate system is given in Figure 3. Here the influence of gravity is not considered.

Murphy and Bradley¹ show that the aerodynamic jump is approximately

$$\theta_j = J_{\tilde{\xi}'} \tilde{\xi}'_0 + J_A (\phi_t / \phi'_\infty) \quad (5)$$

The first term on the right hand side is the jump due to the initial transverse angular momentum given the projectile by the muzzle blast. For the asymmetric projectile, $\tilde{\xi}'_0$ is given by Equation (2). The expression for the coefficient in the first term is¹

$$J_{\tilde{\xi}'} = \frac{I_y}{M_p \ell^2} \frac{C_{L_\alpha}}{C_{M_\alpha}} \quad (6)$$

While the first term in Equation (5) is applicable to both symmetric and asymmetric projectiles launched with an initial angular velocity, the second term involves only the asymmetry of the projectile. Here C_{L_α} , C_{M_α} are the free flight lift and static moment coefficients.

The expression for J_A is

$$J_A = \frac{\rho S \ell}{2 M_p} \left(C_{N_\epsilon} - \frac{C_{L_\alpha} C_{M_\epsilon}}{C_{M_\alpha}} \right) \epsilon e^{i\phi_\epsilon} \quad (7)$$

and

$$\phi_t = f \left(\frac{\phi'_0}{\phi'_\infty}, \frac{\phi'_\infty}{C} \right) \quad ,$$

where

ϕ'_0 = initial free flight roll rate, Equation (3)

ϕ'_∞ = steady state roll rate¹

$$= - C_{\ell_\delta} \delta / [C_{\ell_p} + (I_x / M_p \ell^2) C_D] \quad (8)$$

C = roll damping coefficient¹

$$= - [\rho S \ell / 2 M_p] [(I_x / M_p \ell^2)^{-1} C_{\ell_p} + C_D] \quad (9)$$

C_{ℓ_p} , C_{ℓ_δ} = roll moment coefficients due to roll and fin cant respectively

The expression for ϕ_t will be given and discussed in detail in the next section.

To calculate the total deviation of the projectile from its intended trajectory, one must also consider the transverse linear velocity imparted to the projectile by the muzzle blast. Adding this effect to the aerodynamic jump, one obtains for the total deflection:

$$\Theta = w_o/V_p + J_{\xi'} \xi'_o + (J_A \phi_t/\phi'_\infty) . \quad (10)$$

Using Equation (1) and (2), one obtains

$$\begin{aligned} \Theta = & \left[1 + \frac{C_{L_\alpha}}{C_{M_\alpha}} \frac{\Delta}{l} \right] (\gamma+1) p^* 2A_f \frac{D}{M_p V_p^2} \bar{P} [\epsilon e^{i(\phi_\epsilon + \pi)}] \\ & + J_A [\phi_t/\phi'_\infty] . \end{aligned} \quad (11)$$

IV. APPROXIMATION OF ϕ_t

The expression for ϕ_t is

$$\phi_t = \lim_{s_t \rightarrow \infty} \left(\frac{\phi'_\infty}{Cs_t} \right) \int_0^{s_t} \int_0^{s_{t2}} \exp(i\phi) ds_{t1} ds_{t2} \quad (12)$$

where the roll angle is given as

$$\phi = (\phi'_\infty/C) \{s_t - [(\phi'_o/\phi'_\infty) - 1] [\exp(-s_t) - 1]\} , \quad (13)$$

and

$$s_t = Cs$$

s = distance along the trajectory in calibers.

In this section, a series approximation to ϕ_t (A,B) is given in terms of the parameters:

$$A \equiv \phi'_\infty/C ,$$

$$B \equiv \phi'_o/\phi'_\infty .$$

Murphy and Bradley¹ have shown that the integral in Equation (12) may be transformed to

$$\phi_t(A, B) = iA \int_0^\infty \exp[Af(r)] dr, \quad (14)$$

where

$$f(r) = -\{r + i(B-1)[\exp(-ir)-1]\} \quad (15)$$

They further obtained an expression for $\phi_t(A, 0)$ when A is large:

$$\phi_t(A, 0) = [(1+i)(\pi A)^{1/2}/2] + (i/3) \quad (16)$$

For the current application, it is necessary to consider small, but non-zero, values of B; thus, $\phi_t(A, B)$ is expanded in a Maclaurin series:

$$\phi_t(A, B) \approx \phi_t(A, 0) + \left. \frac{d\phi_t}{dB} \right|_{B=0} B + \frac{1}{2} \left. \frac{d^2\phi_t}{dB^2} \right|_{B=0} B^2 + \dots \quad (17)$$

Differentiating ϕ_t with respect to B, we obtain

$$\frac{d\phi_t}{dB} = A^2 \int_0^\infty [\exp(-ir)-1] \exp[Af(r)] dr \quad (18)$$

Differentiating ϕ_t again, we obtain

$$\frac{d^2\phi_t}{dB^2} = -i A^3 \int_0^\infty [\exp(-ir)-1]^2 \exp[Af(r)] dr \quad (19)$$

For large A and small B, the main contribution to the integral in Equation (14) will occur when r is small. When r is large, the integrand consists of small oscillations about zero, which tend to cancel out in the integration. For B=0, Equation (15) may be expanded in series form:

$$f(r) = - (ir^2/2) - (r^3/6) + (ir^4/24) + (r^5/120) + \dots \quad (20)$$

Using this series, we can write

$$\exp [Af(r)] = [\exp(-iAr^2/2)] \exp (Au), \quad (21)$$

where

$$u = - (r^3/6) + (ir^4/24) + (r^5/120) + \dots \quad (22)$$

In turn, the term $\exp (Au)$ is expanded in series. While Murphy and Bradley needed to consider only two terms in the expansion, Equation (21), to obtain their approximation for $\phi_t (A,0)$, the present authors carried the expansion out to the r^9 term for their approximation to $\phi_t (A,B)$.

Finally, expanding

$$\exp(-ir) - 1 \approx -ir - (r^2/2) + (ir^3/6) + r^4/24, \quad (23)$$

Equations (21) and (23) may be substituted into Equations (17), (18), and (19). By a transformation of variable, we obtain integrals of the form

$$\int_0^{\infty} \eta^m \exp(-i\eta^2) d\eta$$

Integrating this integral around the contour which includes the positive part of the real axis and the line 45° from the real axis, we obtain

$$\int_0^{\infty} \eta^m \exp(-i\eta^2) d\eta = \frac{\exp[-i(m+1)\pi/4]}{2} \Gamma\left(\frac{m+1}{2}\right)$$

where Γ is the well-known gamma function.

By evaluating the gamma function and neglecting negative powers of A , ϕ_t is

$$\begin{aligned} \phi_t = & \{[(1+i)(\pi A)^{1/2}/2] + [i/3]\} + [-A + (2i/3)]B \\ & + \{[(1-i)(\pi A)^{1/2} A/4] - [A/3] + [(1+i)(\pi A)^{1/2}/48] + [2i/135]\}B^2. \end{aligned} \quad (24)$$

This approximate expression for ϕ_t is compared with the exact numerical computations² in Figures 5 and 6. The approximation is quite good up to $B = \pm 0.1$ but fails for greater absolute values of B as A becomes large.

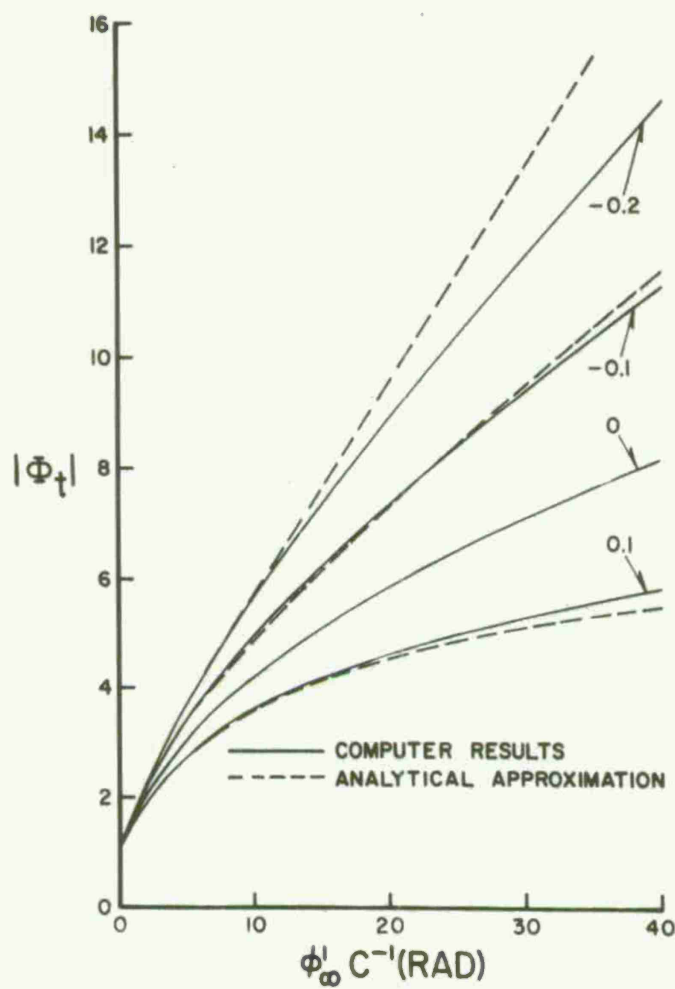


Figure 5. Magnitude of ϕ_t versus $\phi'_\infty C^{-1}$

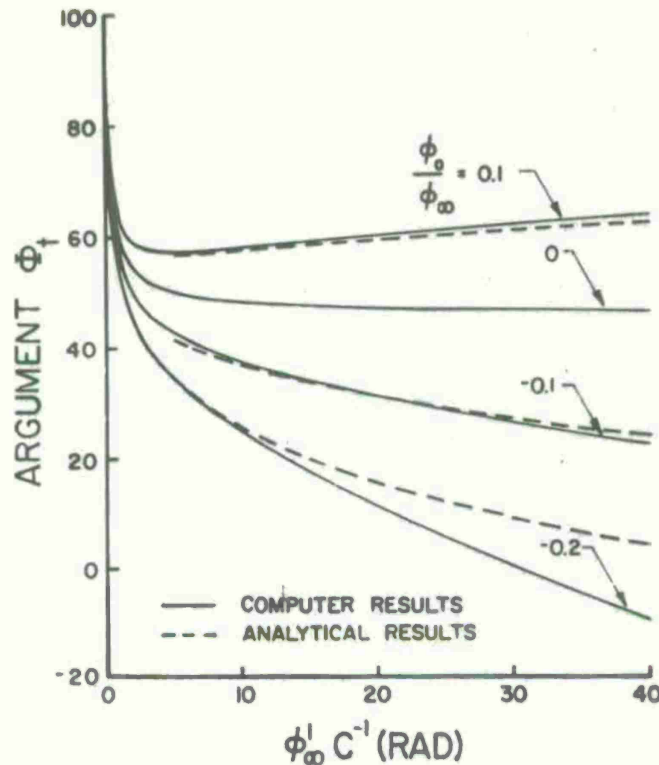


Figure 6. Argument of ϕ_t versus $\phi_\infty' C^{-1}$

In Equation (24), it is apparent that the approximation becomes worse for large A since the leading term in the factor that multiplies B^n is $A^{(n+1)/2}$. The limitation does not affect the analysis since B will seldom have a magnitude greater than 0.1. For instance, the value of B found for a 5.8mm flechette launched from a smoothbore tube is only -0.0403.

V. DEVIATION CAUSED BY MUZZLE BLAST ON ASYMMETRIC PROJECTILES

The total deviation of the projectile is given by Equation (11); however, even if the projectile could be launched in an environment

free of muzzle blast, it would still experience a jump due to asymmetry equal to $J_A [\phi_t(A,0)/\phi_\infty']$. Thus, the contribution of muzzle blast to the total deviation is defined to be:

$$\theta_{mb} = \theta - [J_A \phi_t(A,0)/\phi_\infty'] \quad (25)$$

From Equation (24), the lead terms of $\phi_t - \phi_t(A,0)$ are

$$\begin{aligned} \phi_t - \phi_t(A,0) &\approx -AB \{1 - [2i/(3A)] - [(1-i)(\pi A)^{1/2} B/4]\} \\ &\equiv -ABT. \end{aligned} \quad (26)$$

Thus, from Equation (7) and (11)

$$\begin{aligned} \theta_{mb} &= [1 + \frac{C_{L\alpha}}{C_{M\alpha}} \frac{\Delta}{\ell}] (\gamma+1) p^* 2 A_f \frac{D}{M_p V_p^2} \bar{p} [\epsilon e^{i(\phi_\epsilon + \pi)}] \\ &\quad - \frac{\rho S \ell}{2M_p} C_{N_\epsilon} (1 - \frac{C_{L\alpha}}{C_{M\alpha}} \frac{C_{M_\epsilon}}{C_{N_\epsilon}}) \epsilon e^{i\phi_\epsilon} \frac{ABT}{\phi_\infty'} \quad (27) \end{aligned}$$

According to linear theory,²

$$\frac{C_{M_\epsilon}}{C_{N_\epsilon}} = - \frac{\Delta_\epsilon}{\ell},$$

where

$$\begin{aligned} \Delta_\epsilon &= \text{c.g. - c.p. separation of asymmetric fin} \\ &\approx \Delta. \end{aligned}$$

Substituting into Equation (27),

$$\begin{aligned} \theta_{mb} &= - [1 + \frac{C_{L\alpha}}{C_{M\alpha}} \frac{\Delta}{\ell}] \epsilon e^{i\phi_\epsilon} \{ (\gamma+1) p^* 2 A_f \frac{D}{M_p V_p^2} \bar{p} \\ &\quad + \frac{\rho S \ell}{2M_p} C_{N_\epsilon} \frac{ABT}{\phi_\infty'} \} \quad (28) \end{aligned}$$

Examine the right hand term within the braces in Equation (28):

$$\Psi \equiv \frac{\rho S l}{2 M_p} C_{N_\epsilon} \frac{ABT}{\phi'_\infty} = \frac{\rho S l}{2 M_p} C_{N_\epsilon} \frac{1}{C} \frac{\phi'_0}{\phi'_\infty} T \quad (29)$$

From Equations (8) and (9),

$$C \phi'_\infty = C_{\ell_\delta} \delta \ell^2 (\rho S l) / (2 I_x), \quad (30)$$

yielding:

$$\Psi = \frac{I_x}{M_p \delta \ell^2} \frac{C_{N_\epsilon}}{C_{\ell_\delta}} \phi'_0 T. \quad (31)$$

Again, according to linear theory,²

$$\frac{C_{N_\epsilon}}{C_{\ell_\delta}} = \frac{2}{n} \frac{\ell}{r_o}. \quad (32)$$

Substitution of Equations (3) and (32) into Equation (31) yields

$$\Psi = - (\gamma+1) p^* 2 A_f \frac{D}{M_p V_p^2} \bar{P} T. \quad (33)$$

Equation (28) becomes:

$$\Theta_{mb} = - \left\{ \left[1 + \frac{C_{L_\alpha}}{C_{M_\alpha}} \frac{\Delta}{\ell} \right] (\gamma+1) p^* 2 A_f \frac{D}{M_p V_p^2} \bar{P} \right\} [1-T] \epsilon e^{i \phi_\epsilon} \quad (34)$$

The quantity in the left hand brace is identical to the coefficient in the deflection equation² describing the muzzle-blast-induced deviation of a symmetric projectile launched at an angle of attack, $\tilde{\xi}_m$. Hence, by evaluating the magnitude of $1-T$, a direct comparison can be made between the sensitivity of symmetric and asymmetric projectiles to muzzle blast. From Equation (26),

$$1 - T = [2i/(3A)] + [(1-i) (\pi A)^{1/2} B/4].$$

The value of A is frequently near 25 while B is on the order of 0.05; thus, the magnitude of $1-T$ is approximately 0.1. Since a typical muzzle blast deviation of a symmetric projectile is on the order of 0.1 mil deflection per degree of initial angle of attack, the sensitivity of the asymmetrical projectile would be about 0.01 mil deflection per degree of asymmetric fin deflection.

VI. SUMMARY AND CONCLUSIONS

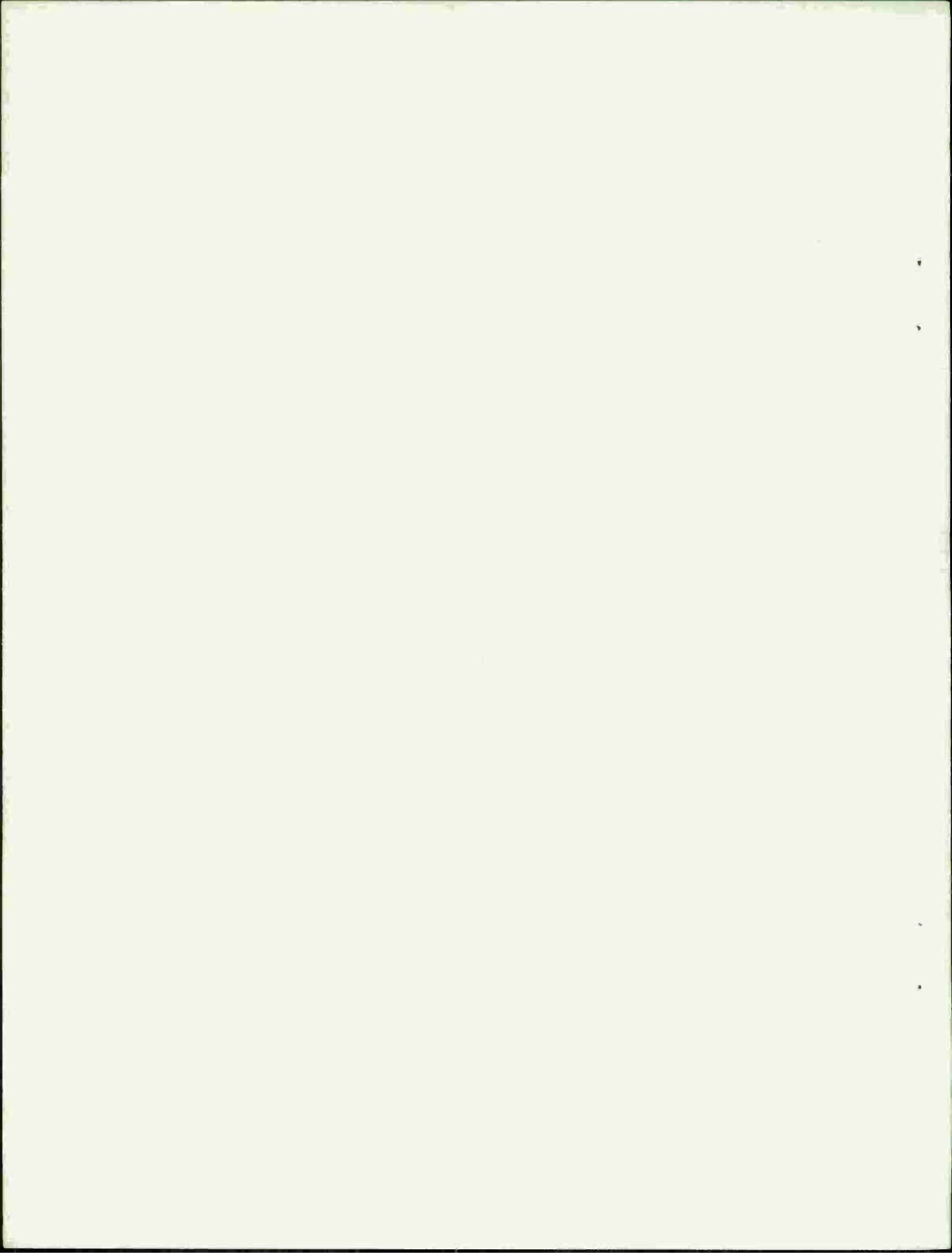
Using a simple approximation, a closed form expression for the effect of muzzle blast on the jump due to asymmetry of fin-stabilized projectiles is obtained. The analysis shows that muzzle blast does not significantly alter this portion of the total jump.

ACKNOWLEDGEMENT

The authors wish to thank Mr. James Bradley of the Exterior Ballistics Laboratory for his assistance in this analysis.

REFERENCES

1. Murphy, C. H. and Bradley, J. W., "Jump Due to Aerodynamic Asymmetry of a Missile with Varying Roll Rate," BRL R 1077, U. S. Army Ballistic Research Laboratories, Aberdeen Proving Ground, Maryland, May 1959, AD 219312.
2. Fansler, K.S. and Schmidt, E. M., "The Influence of Muzzle Gasdynamics upon the Trajectory of Fin-Stabilized Projectiles," BRL R 1793, U.S. Army Ballistic Research Laboratories, Aberdeen Proving Ground, Maryland, June 1975, AD B005379L.
3. Oswatitsch, K., "Intermediate Ballistics," Deutsche Luft und Raumfahrt FB 64-37, DVL Bericht 358, December 1964, AD 473249.
4. Gretler, W., "Intermediate Ballistics Investigations of Wing Stabilized Projectiles," German Air and Space Research Report 67-92, FSTC-HT-23-22-69-72, 1967.



LIST OF SYMBOLS

A_f	planform area of single fin
c	local sound speed
C	roll damping coefficient
C_{ℓ_p}	roll moment coefficient due to roll
C_{ℓ_δ}	roll moment coefficient due to fin cant
C_L, C_{L_α}	projectile lift coefficient and derivative with respect to α
C_{M_α}	projectile static moment coefficient
C_{M_ϵ}	moment coefficient due to fin deflection
C_{N_ϵ}	normal force coefficient due to fin deflection
d	distance from obturator to fin c.p.
D	diameter of gun bore
I_x, I_y	longitudinal and transverse moments of inertia
$J_A, J_{\tilde{\xi}}, J_{\tilde{\xi}}'$	jump coefficients
ℓ	shaft diameter of projectile
\bar{L}	dimensionless fin lift function
M	Mach number or moment
M_p	mass of the projectile
n	number of fins
p	pressure
\bar{p}	dimensionless momentum function
\bar{p}_o, \bar{p}_b	muzzle jet and in-bore momentum impulse
s	distance along trajectory in calibers ($s = x_e/\ell$)
S	reference area of projectile ($S = \pi\ell^2/4$)
t	time ($t=0$ corresponds to obturator passing muzzle)

LIST OF SYMBOLS (Continued)

V_p	projectile velocity
w	transverse velocity in Z_e direction
X, Y, Z	coordinates
$\tilde{\alpha}, \tilde{\beta}$	angles of attack and sideslip in non-rolling coordinate system
γ	ratio of specific heats
δ	differential fin cant angle
Δ, Δ_f	c.p. - c.g. separation in reverse and forward flow, respectively
ϵ	magnitude of asymmetric fin cant angle
$\tilde{\xi}$	complex angle of yaw $\tilde{\beta} + i \tilde{\alpha}$
θ	angular deflection of projectile from boreline
θ_j	aerodynamic jump: angular deflection from particle trajectory (gravity and drag determined) due to aerodynamic forces
θ_{mb}	angular deflection of projectile due to muzzle blast
ρ	density
ϕ	roll angle
ϕ_ϵ	initial, free flight orientation of asymmetric fin force

Subscripts

e	denotes earth-fixed coordinates
o	denotes projectile properties immediately after penetration of the muzzle blast
∞	denotes ambient or steady state conditions

Superscripts

$(\bar{})$	denotes dimensionless quantities
$()'$	denotes derivative with respect to s
$()^*$	denotes critical or sonic conditions

DISTRIBUTION LIST

<u>No. of Copies</u>	<u>Organization</u>	<u>No. of Copies</u>	<u>Organization</u>
2	Commander Defense Documentation Center ATTN: DDC-TCA Cameron Station Alexandria, VA 22314	1	Commander US Army Tank Automotive Development Command ATTN: DRDTA-RWL Warren, MI 48090
1	Director Defense Nuclear Agency Washington, DC 20305	2	Commander US Army Mobility Equipment Research & Development Command ATTN: Tech Docu Cen, Bldg. 315 DRSME-RZT Fort Belvoir, VA 22060
1	Commander US Army Materiel Development Readiness Command ATTN: DRCDMA-ST 5001 Eisenhower Avenue Alexandria, VA 22333	3	Commander US Army Armament Command ATTN: P. Ehle E. Haug Tech Lib Rock Island, IL 61202
1	Commander US Army Aviation Systems Command ATTN: DRSAB-E 12th and Spruce Streets St. Louis, MO 63166	2	Commander US Army Armament Command ATTN: Rodman Laboratories S. Thompson S. Burley Rock Island, IL 61202
1	Director US Army Air Mobility Research and Development Laboratory Ames Research Center Moffett Field, CA 94035	6	Commander US Army Frankford Arsenal ATTN: Mr. T. Boldt SARFA-U2100 Mr. J. Mitchell SARFA-U3100, S. Fulton SARFA-U3300 Mr. S. Hirshman Mr. A. Cianciosi L4100-150-2 Mr. C. Sleischer, Jr. Philadelphia, PA 19137
1	Commander US Army Electronics Command ATTN: DRSEL-RD Fort Monmouth, NJ 07703		
1	Commander US Army Missile Command ATTN: DRSMI-R Redstone Arsenal, AL 35809		
5	Commander US Army Missile Command ATTN: DRSMI-RDK, R. Deep R. Becht (4 Cys) Redstone Arsenal, AL 35809		

DISTRIBUTION LIST

<u>No. of</u> <u>Copies</u>	<u>Organization</u>	<u>No. of</u> <u>Copies</u>	<u>Organization</u>
9	Commander US Army Picatinny Arsenal ATTN: SARPA-DR-D, S.Wasserman SARPA-DR-V, Mr. A.Loeb Mr. D. Mertz Mr. E. Friedman SARPA-D, Mr. Lindner SARPA-V, E. Walbrecht Mr. S. Verner SARPA-VE, Dr. Kaufman SARPA-FR-M-MA Mr. E. Barrieres Dover, NJ 07801	1	Commander US Army Research Office ATTN: CRD-AA-EH P. O. Box 12211 Research Triangle Park, NC 27709
2	Commander US Army Watervliet Arsenal ATTN: Tech Lib SARWV-PDR-S, F. Sautter Watervliet, NY 12189	1	Commander US Army Ballistic Missile Defense Systems Command Huntsville, AL 35804
1	Commander US Army Harry Diamond Labs ATTN: DRXDO-TI 2800 Powder Mill Road Adelphi, MD 20783	1	Director US Army Advanced BMD Technology Center P.O. Box 1500, West Station Huntsville, AL 35809
1	Director US Army TRADOC Systems Analysis Activity ATTN: ATAA-SA White Sands Missile Range NM 88002	3	Commander US Naval Air Systems Command ATTN: AIR-604 Washington, DC 20360
1	Commander US Army Materials and Mechanics Research Center ATTN: DRXMR-ATL Watertown, MA 02172	3	Commander US Naval Ordnance Systems Command ATTN: ORD-9132 Washington, DC 20360
1	Commander US Army Natick Research and Development Center ATTN: DRXRE, Dr. D. Sieling Natick, MA 01762	2	Commander and Director David W. Taylor Naval Ship Research & Development Center ATTN: Tech Lib Aerodynamic Lab Bethesda, MD 20084
		3	Commander US Naval Surface Weapons Center ATTN: Code 312, Mr. F. Ragan Mr. S. Hastings Code 730, Tech Lib Silver Spring, MD 20910

DISTRIBUTION LIST

<u>No. of</u> <u>Copies</u>	<u>Organization</u>	<u>No. of</u> <u>Copies</u>	<u>Organization</u>
3	Commander US Naval Surface Weapons Center ATTN: Code GX, Dr. W. Kemper Mr. F. H. Maille Dr. G. Moore Dahlgren, VA 22448	1	Director NASA Scientific and Technical Information Facility ATTN: SAK/DL P. O. Box 8757 Baltimore/Washington International Airport, MD 21240
1	Commander US Naval Weapons Center ATTN: Code 553, Tech Lib China Lake, CA 93555	1	Director Jet Propulsion Laboratory ATTN: Tech Lib 2800 Oak Grove Drive Pasadena, CA 91103
3	Director US Naval Research Laboratory ATTN: Tech Info Div Code 7700, D. A. Kolb Code 7720, Dr. E. McClean Washington, DC 20390	2	Director National Aeronautics and Space Administration George C. Marshall Space Flight Center ATTN: MS-1, Lib R-AERO-AE, A. Felix Huntsville, AL 35812
1	Commander US Naval Ordnance Station ATTN: Code FS13A, P. Sewell Indian Head, MD 20640	1	Director National Aeronautics and Space Administration Langley Research Center ATTN: MS 185, Tech Lib Langley Station Hampton, VA 23365
2	ADTC (ADBPS-12) Eglin AFB, FL 32542	1	Advanced Technology Labs ATTN: Dr. J. Erdos Merrick & Stewart Avenues Westbury, NY 11590
1	AFATL (DLDG) Eglin AFB, FL 32542	2	ARO, Inc. ATTN: Tech Lib Arnold AFS, TN 37389
1	AFATL (DLY) Eglin AFB, FL 32542	1	Technical Director Colt Firearms Corporation 150 Huyshore Avenue Hartford, CT 14061
1	AFATL (DLDL, Dr. D.C. Daniel) Eglin AFB, FL 32542		
2	AFATL (DLRA, F. Burgess; Tech Lib) Eglin AFB, FL 32542		
1	AFWL (DEV) Kirtland AFB, NM 87117		
1	ASD (ASBEE) Wright-Patterson AFB, OH 45433		

DISTRIBUTION LIST

<u>No. of Copies</u>	<u>Organization</u>	<u>No. of Copies</u>	<u>Organization</u>
1	General Electric Corporation Armaments Division ATTN: Mr. R. Whyte Lakeside Avenue Burlington, VT 05401	1	Massachusetts Institute of Technology Dept of Aeronautics and Astronautics ATTN: Tech Lib 77 Massachusetts Avenue Cambridge, MA 02139
1	Northrop Corporation Aircraft Division ATTN: Dr. A. Wortman 3901 W. Broadway Hawthorne, CA 90250	1	Ohio State University Dept of Aeronautics and Astronautical Engineering ATTN: Tech Lib Columbus, OH 43210
1	Winchester-Western Division Olin Corporation ATTN: Mr. D. Merrill New Haven, CT 06504	1	Polytechnic Institute of Brooklyn Graduate Center ATTN: Tech Lib Farmingdale, NY 11735
1	Sandia Laboratories ATTN: Aerodynamics Dept Org 5620, R. Maydew P. O. Box 5800 Albuquerque, NM 87115	1	Director Forrestal Research Center Princeton University Princeton, NJ 08540
1	Guggenheim Aeronautical Lab California Inst of Technology ATTN: Tech Lib Pasadena, CA 91104	1	Princeton University Forrestal Laboratories ATTN: Dr. M. Summerfield Princeton, NJ 08540
1	Calspan Corporation ATTN: Mr. G. A. Sterbutzel P. O. Box 235 Buffalo, NY 14221	1	Southwest Research Institute ATTN: Mr. Peter S. Westine P. O. Drawer 28510 8500 Culebra Road San Antonio, TX 78228
2	Franklin Institute ATTN: Dr. Carfagno Dr. Wachtell Race & 20th Streets Philadelphia, PA 19103		<u>Aberdeen Proving Ground</u> Marine Corps Ln Ofc Dir, USAMSAA
1	The Johns Hopkins University Applied Physics Laboratory Johns Hopkins Road Laurel, MD 20810		

